

A DUAL-SCALE LEAD-SEPARATED TRANSFORMER WITH LEAD-ORTHOGONAL ATTENTION AND META-INFORMATION FOR ECG CLASSIFICATION

Yang Li¹, Guijin Wang¹, Zhouhui Xia², Wenming Yang³, Li Sun^{1*}

¹Department of Electronic Engineering, Tsinghua University, Beijing 100084, China,

²Huachuang Aima Information Technology, Chengdu 610094, China, ³Department of Electronic Engineering, Tsinghua Shenzhen International Graduate School, Shenzhen 518055, China

ABSTRACT

Auxiliary diagnosis of cardiac electrophysiological status can be obtained through the analysis of 12-lead electrocardiograms (ECGs). This work proposes a dual-scale lead-separated transformer with lead-orthogonal attention and meta-information (DLTM-ECG) as a novel approach to address this challenge. ECG segments of each lead are interpreted as independent patches, and together with the reduced dimension signal, they form a dual-scale representation. As a method to reduce interference from segments with low correlation, two group attention mechanisms perform both lead-internal and cross-lead attention. Our method allows for the addition of previously discarded meta-information, further improving the utilization of clinical information. Experimental results show that our DLTM-ECG yields significantly better classification scores than other transformer-based models, matching or performing better than state-of-the-art (SOTA) deep learning methods on two benchmark datasets. Our work has the potential for similar multichannel bioelectrical signal processing and physiological multimodal tasks.

Index Terms— transformer, electrocardiogram, arrhythmia classification

1. INTRODUCTION

Cardiovascular disease (CVD) remains a leading cause of death worldwide, greatly necessitating improvements in the quality and quantity of care [1]. Cardiac electrophysiological recordings have become fundamental for discerning cardiac symptomology in patients, and a plethora of information can be examined through the interpretation of 12-lead electrocardiograms (ECGs). More accessible medical services and the widespread use of wearable ECG monitoring devices have greatly increased the availability of ECG data for clinicians, but simultaneously it has become impossible for cardiologists to manually interpret the massive amounts of data generated in these scenarios.

In recent years, automatic ECG diagnostic technology has been developed based on custom-built deep learning models

such as Convolution Neural Networks (CNNs), Long Short-Term Memory networks (LSTMs), and transformer-based networks [2, 3, 4, 5], some of which report current state-of-the-art (SOTA) scores. Currently, researchers involved with automated ECG diagnostics are paying increased attention to transformer-based models which have performed very well in a variety of fields due to transformers' advantages in capturing long-range attention and ability to encode input with various semantics [6, 7]. In a recent study, CNN layers and transformer layers extracted information directly from ECG segments, and 20 of 300 features designed by experts were selected including heart rate variability and morphological features [8]. BaT regards the aligned heartbeat sequence as input and aggregates all heartbeat features with the convolution layer after 1D Swin transformer blocks [4].

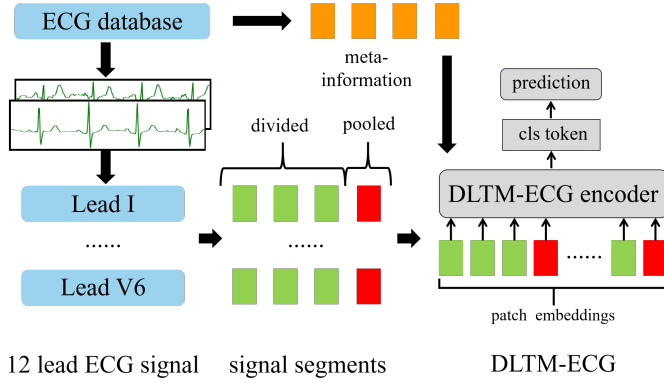
In this work, we propose a novel lead-separated transformer with meta-information called DLTM-ECG, with dual-scale representation and lead-orthogonal attention mechanisms. In this proposed neural network, the one-dimensional multichannel ECG input is first subdivided into patches by time and lead, then concatenated with reduced-dimension features to obtain dual-scale information. We adopt not only vanilla attention but also lead-orthogonal attention mechanisms. To adaptively integrate information from all feature tokens, the global average pooling (GAP) of features serves as the initialization of the class token. The meta-information from the ECG database is encoded and adopted to facilitate comprehensive learning about the representation of different types of information. Experimental results show that our method is significantly improved over the previous ECG transformer structure and matches or performs better than the previous state-of-the-art (SOTA) methods in multiple tasks.

2. METHODOLOGY

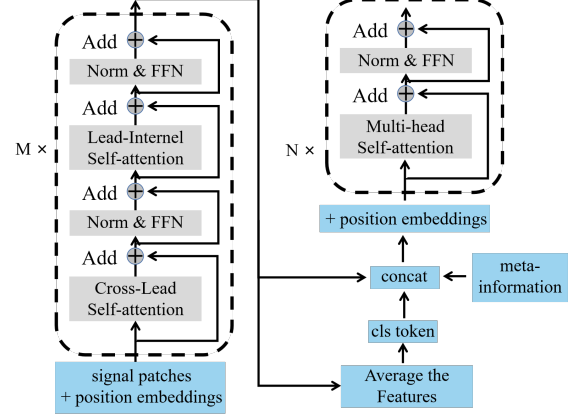
2.1. Model structure

Fig. 1 shows the overall structure of the proposed model. We obtained both ECG signals and meta-information from public databases. Input ECG is divided by time and lead. The signal from each lead is pooled to obtain reduced-dimension

*Corresponding author: sunli_3595@163.com.



(a) Input signal is embedded to patches as input.



(b) Encoder structure.

Fig. 1. Overview of DLTM-ECG method.

Table 1. Model hyperparameters.

Input size	(12, 250)
ECG segment length	50
Embedding dimension	160
Hidden dimension	480
Number of lead-orthogonal attention blocks	4
Number of MSA blocks	2
Number of heads	5

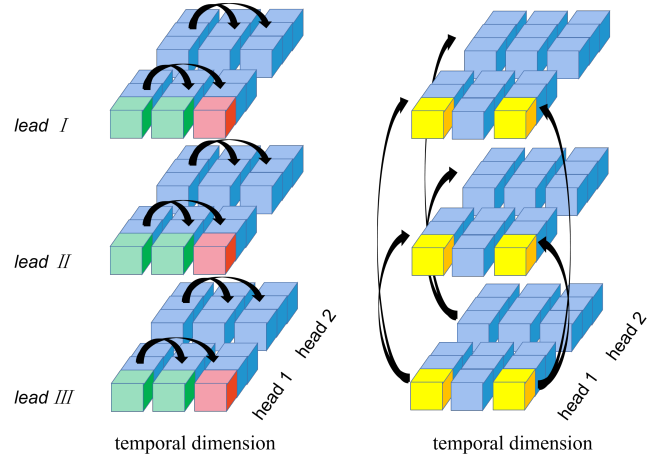
features with a coarse scale which, together with the original signal, constitutes a dual-scale representation. The initial few layers of the model adopted lead-orthogonal attention modules to define the computational range of attention and reduce interference from segments with low correlation. The global information is then integrated in transformer layers with vanilla attention. **Table 1** shows some model hyperparameters. DLTM-ECG has 2.6M trainable parameters. Code will be available.

2.2. Lead-separated ECG segmentation on dual scales

Different ECG leads are regarded by cardiologists as diverse perspectives of cardiac electrical activity [9]. Our transformer-based model is expected to notice diversity among various ECG leads, hence we proposed a lead-separated division method. Specifically, a segment from one single channel is treated as a patch. At the same time, since it is difficult for transformer blocks to synthesize information at different scales, we pooled ECG signals in the time dimension to introduce both coarse and fine-grained scales. As a

commonly used method to reduce feature dimension, maximum pooling could retain peak and elevation information and demonstrate sufficient effectiveness in our experiments. All patches are linearly projected into patch embeddings as inputs of the DLTM-ECG encoder. We used 12-lead ECG as an example in this work, but due to the transformer’s flexibility in the number of input patch embeddings, our model can support records with a variable number of leads.

2.3. Multiple attention calculation mechanisms



(a) Lead-internal self-attention. (b) Cross-lead self-attention.

Fig. 2. Lead-orthogonal attention mechanism.

Based on the above segmentation and pooling procedure, our model is built on both vanilla self-attention blocks and novel lead-orthogonal attention blocks [10, 11]. The vanilla multihead self-attention (MSA) blocks are cascaded after the lead-orthogonal attention blocks. Our lead-orthogonal atten-

tion module includes lead-internal multihead self-attention and cross-lead multihead self-attention as shown in **Fig. 2**. It has a clear physical meaning with each group naturally corresponding to segments within the same lead or time period. In the lead-internal multihead self-attention, we treated all tokens of different leads at the same time, whether they are from initial records or pooled records, as a group. Correspondingly, in the cross-lead multihead self-attention, we treated all tokens in the same lead as a group.

The group multi-head self-attention in the dual attention block can be represented by

$$A_{group}(Q, K, V) = \{A_{Mhead}(Q_i, K_i, V_i)\}_{i=0}^{N_{group}} \quad (1)$$

where attention in a single group is:

$$A_{Mhead}(Q_i, K_i, V_i) = \text{Concat} \{head_j\}_{group=i}^{j \in [1, N_{head}]} \quad (2)$$

and for each attention head:

$$head_j = \text{softmax} \left(\frac{Q_j K_j^T}{\sqrt{d_h}} \right) V_j \quad (3)$$

2.4. Fusion of meta-information

Previous studies in the field of image classification have shown that the effective use of meta-information can improve the knowledge extraction ability of the model[12]. The transformer has the advantage of being able to flexibly adapt to the various input information, thus allowing for intuitive integration of previously discarded meta-information into the proposed model. The meta-information embeddings, combined with the output features of the lead-orthogonal attention layers and the class token, become the input of the following vanilla attention layers.

3. EXPERIMENTS

3.1. Datasets and preprocessing

PTB-XL is a publicly available clinical dataset containing 21,837 records of 12-lead ECG dataset from 18,885 patients with a 10-second duration [13]. Each record states whether the recording belongs to one or more multi-label classification tasks including ‘all’, ‘diagnostic’, ‘superdiagnostic’, ‘subdiagnostic’, ‘rhythm’ and ‘form’. Meta-information including age, gender, height and weight is available.

Chapman is another open-source clinical database comprised of 12-lead ECG signals from 10646 individuals. Age and gender are available in this dataset [14]. The labels of all data are clustered into four disjoint categories SR, SB, GSVT, and AFIB. Both the original and denoised versions are provided. We trained on both original and denoised records and tested only on original records.

We selected the 100Hz version for both datasets. For PTB-XL, according to the recommended partition, eight of

Table 2. Ablation study results(%).

Lead independence	Dual scale	Multiple attention	Meta-information	macro AUC
×	×	×	×	91.6
✓	×	×	×	92.6
✓	✓	×	×	92.9
✓	×	✓	×	92.8
✓	✓	✓	×	93.4
✓	✓	✓	✓	94.2

the 10 folds are used for training, one for validation and the other for testing. For Chapman, we implemented 10 fold cross-validation with 80% indices for training, 10% for validation and 10% for testing.

3.2. Evaluation metrics

The comparison with current methods on PTB-XL dataset was achieved through the macro-AUC, which measures class separability by calculating the area under the receiver operating characteristic curve for each label and then averaging them. For the Chapman database, we further adopted the following metrics: accuracy, macro-precision, macro-recall and macro-F1. For each class we have

$$Precision = \frac{TP}{TP + FP} \quad (4)$$

$$Recall = \frac{TP}{TP + FN} \quad (5)$$

$$F1 = \frac{2 * Recall * Precision}{Recall + Precision} \quad (6)$$

The macro metrics calculates the average of results for each class.

3.3. Implementation details

In each training step, a sliding window with a random offset generates segments from the current batch data, and DLTM-ECG iterates over the segments in turn. This avoids unstable training caused by excessive randomness and alleviates inefficiencies caused by the transformer’s lack of inductive bias to spatial invariance. We warmed up the model for 20 epochs at a linear schedule and then applied ReduceLROnPlateau learning rate schedule, which automatically halves the learning rate when the validation score doesn’t improve. The max learning rate was set to 0.003, and the batch size is set to 128 for both datasets. An Adamw optimizer with $\beta_1 = 0.9$, $\beta_2 = 0.99$ and weight decay = 0.05 was applied as our base optimizer. Then we wrapped the base optimizer with the SAM method, and the radius of hypersphere ρ was set to 0.05 [19]. An exponential moving average (EMA)[20] with $\alpha = 0.998$ is implemented, and the shadow weight is updated after each training step. BCEWithLogits loss function is used.

Table 3. Experimental results(%) on PTB-XL.

method	all	diag	superdiag	subdiag	rhythm	form
Wavelet+NN [3]	84.9	85.5	87.4	85.9	89.0	75.7
LSTM [3]	90.7	92.7	92.7	92.8	95.3	85.1
LSTM_bidir [3]	91.4	93.2	92.1	92.3	94.9	87.6
CNN+LSTM [5]	93.2	93.2	92.9	92.9	95.0	89.2
resnet1d [3]	91.9	93.6	93.0	92.8	94.6	88.0
method in [15]	-	-	93.1	-	-	-
ST-CNN-GAP-5 [16]	-	-	93.4	-	-	-
fcn [3]	91.8	92.6	92.5	92.7	93.1	86.9
IMLE-Net [2]	-	-	92.2	-	-	-
inception1d [3]	92.5	93.1	92.1	<u>93.0</u>	95.3	<u>89.9</u>
xresnet1d [3]	92.5	<u>93.7</u>	92.8	92.9	95.7	89.6
multi-period attention [17]	92.7	93.1	93.0	92.3	97.2	85.2
ViT [4]	86.2	-	-	-	-	-
BaT [4]	90.5	-	-	-	-	-
DLTM-ECG	94.2	93.9	<u>93.2</u>	93.8	<u>96.1</u>	91.7

Table 4. Experimental results(%) on Chapman.

metric	[18]	[16]	DLTM-ECG
accuracy	96.1	96.2	96.3
macro precision	95.8	95.9	96.2
macro recall	95.4	95.7	95.7
macro F1	95.6	95.8	95.9
macro AUC	-	99.5	99.7

3.4. Ablation study

We provided ablation experiments on the most fine-grained task of PTB-XL. Except for ablation variables, other training settings remained the same. For meta-information ablation, we simply removed these tokens. For multi-attention ablation, we replaced lead-orthogonal attention blocks with double numbers of multihead self-attention blocks that have a similar number of parameters. To remove the dual scale, we skipped the pooling step. We ablated the independence of different leads in this way: instead of dividing 50 points (i.e. 0.5 seconds) off one lead into one patch, we took the 12-channel record of 0.05 seconds as the basic unit, which divides the record temporally and keeps a similar number of patch embeddings. Ablation results shown in **Table 2** demonstrate the effectiveness of each innovation we propose.

3.5. Comparison with the state-of-the-arts

The evaluation results on PTB-XL are shown in **Table 3** together with current SOTA methods. A previous approach provides benchmarking results covering models including LSTM_bidir, inception1d and xresnet1d [3]. Periodic masks were introduced in [17] to better capture rhythm informa-

tion. Non-local convolutional block attention module was used in [17] to capture long-range correlation. Both spatial and temporal layers were adopted in [16] which lead to a diagnostic model with decent performance. The work in [5] combines CNN and LSTM and generalizes well on multiple tasks. We run our experiment 10 times and report the average macro-AUC for each task. Our approach achieved the most advanced overall performance on multiple tasks and exceeded the baseline ViT [4] by 8% with an AUC score of 94.2%. Even without the addition of meta-information, the model still obtains well performance, which proves the effectiveness of our method for feature extraction. We also list the results of the SOTA end-to-end deep learning methods using Chapman in **Table 4** together with our experimental results under the same settings as PTB-XL. Our method shows good generalization performance in multiple metrics and obtains scores matching or performing better than compared models.

4. CONCLUSION

In this work we present a transformer-based model DLTM-ECG to classify clinical ECG records. We considered characteristics of the transformer and ECG signals to design specific structures. Lead-separated segmentation was proposed to capture the correlation between leads, and the signal was pooled to obtain dual-scale representation. Multiple attention mechanisms further improved the feature extraction ability. The incorporation of meta-information into the model is an important innovation that not only improves classification scores but also reveals the potential to utilize multimodal data in a variety of different physiological signal analyses. Classification results on multiple tasks and ablation experiments have confirmed the effectiveness of the proposed technology.

5. REFERENCES

- [1] Theo Vos, Stephen S Lim, Cristiana Abbafati, Kaja M Abbas, Mohammad Abbasi, Mitra Abbasifard, Mohsen Abbasi-Kangevari, Hedayat Abbastabar, Foad Abd-Allah, Ahmed Abdelalim, et al., “Global burden of 369 diseases and injuries in 204 countries and territories, 1990–2019: a systematic analysis for the global burden of disease study 2019,” *The Lancet*, vol. 396, no. 10258, pp. 1204–1222, 2020.
- [2] Likith Reddy, Vivek Talwar, Shanmukh Alle, Raju S Bapi, and U Deva Priyakumar, “Imle-net: An interpretable multi-level multi-channel model for ecg classification,” in *2021 IEEE International Conference on Systems, Man, and Cybernetics (SMC)*. IEEE, 2021, pp. 1068–1074.
- [3] Nils Strodthoff, Patrick Wagner, Tobias Schaeffter, and Wojciech Samek, “Deep learning for ecg analysis: Benchmarks and insights from ptb-xl,” *IEEE Journal of Biomedical and Health Informatics*, vol. 25, no. 5, pp. 1519–1528, 2020.
- [4] Xiaoyu Li, Chen Li, Yuhua Wei, Yuyao Sun, Jishang Wei, Xiang Li, and Buyue Qian, “Bat: Beat-aligned transformer for electrocardiogram classification,” in *2021 IEEE International Conference on Data Mining (ICDM)*. IEEE, 2021, pp. 320–329.
- [5] Temesgen Mehari and Nils Strodthoff, “Self-supervised representation learning from 12-lead ecg data,” *Computers in biology and medicine*, vol. 141, pp. 105114, 2022.
- [6] Ashish Vaswani, Noam Shazeer, Niki Parmar, Jakob Uszkoreit, Llion Jones, Aidan N Gomez, Łukasz Kaiser, and Illia Polosukhin, “Attention is all you need,” *Advances in neural information processing systems*, vol. 30, 2017.
- [7] Arsha Nagrani, Shan Yang, Anurag Arnab, Aren Jansen, Cordelia Schmid, and Chen Sun, “Attention bottlenecks for multimodal fusion,” *Advances in Neural Information Processing Systems*, vol. 34, 2021.
- [8] Annamalai Natarajan, Yale Chang, Sara Mariani, Asif Rahman, Gregory Boverman, Shruti Vij, and Jonathan Rubin, “A wide and deep transformer neural network for 12-lead ecg classification,” in *2020 Computing in Cardiology*. IEEE, 2020, pp. 1–4.
- [9] Wenhan Liu, Qijun Huang, Sheng Chang, Hao Wang, and Jin He, “Multiple-feature-branch convolutional neural network for myocardial infarction diagnosis using electrocardiogram,” *Biomedical Signal Processing and Control*, vol. 45, pp. 22–32, 2018.
- [10] Mingyu Ding, Bin Xiao, Noel Codella, Ping Luo, Jingdong Wang, and Lu Yuan, “Davvit: Dual attention vision transformers,” *arXiv preprint arXiv:2204.03645*, 2022.
- [11] Xiaoyi Dong, Jianmin Bao, Dongdong Chen, Weiming Zhang, Nenghai Yu, Lu Yuan, Dong Chen, and Baining Guo, “Cswin transformer: A general vision transformer backbone with cross-shaped windows,” in *CVPR*, 2022, pp. 12124–12134.
- [12] Qishuai Diao, Yi Jiang, Bin Wen, Jia Sun, and Zehuan Yuan, “Metaformer: A unified meta framework for fine-grained recognition,” *arXiv preprint arXiv:2203.02751*, 2022.
- [13] Patrick Wagner, Nils Strodthoff, Ralf-Dieter Boussejot, Dieter Kreiseler, Fatima I Lunze, Wojciech Samek, and Tobias Schaeffter, “Pt看-xl, a large publicly available electrocardiography dataset,” *Scientific data*, vol. 7, no. 1, pp. 1–15, 2020.
- [14] Jianwei Zheng, Jianming Zhang, Sidy Danioko, Hai Yao, Hangyuan Guo, and Cyril Rakovski, “A 12-lead electrocardiogram database for arrhythmia research covering more than 10,000 patients,” *Scientific Data*, vol. 7, no. 1, pp. 1–8, 2020.
- [15] Jikuo Wang, Xu Qiao, Changchun Liu, Xinpei Wang, YuanYuan Liu, Lianke Yao, and Huan Zhang, “Automated ecg classification using a non-local convolutional block attention module,” *Computer Methods and Programs in Biomedicine*, vol. 203, pp. 106006, 2021.
- [16] Atul Anand, Tushar Kadian, Manu Kumar Shetty, and Anubha Gupta, “Explainable ai decision model for ecg data of cardiac disorders,” *Biomedical Signal Processing and Control*, vol. 75, pp. 103584, 2022.
- [17] Xulu Zhang and Kai Zhou, “Multi-period attention for automatic ecg classification,” in *ICMLCA 2021; 2nd International Conference on Machine Learning and Computer Application*. VDE, 2021, pp. 1–4.
- [18] Ozal Yildirim, Muhammed Talo, Edward J Ciaccio, Ru San Tan, and U Rajendra Acharya, “Accurate deep neural network model to detect cardiac arrhythmia on more than 10,000 individual subject ecg records,” *Computer methods and programs in biomedicine*, vol. 197, pp. 105740, 2020.
- [19] Pierre Foret, Ariel Kleiner, Hossein Mobahi, and Behnam Neyshabur, “Sharpness-aware minimization for efficiently improving generalization,” *arXiv preprint arXiv:2010.01412*, 2020.
- [20] Kaiming He, Xinlei Chen, Saining Xie, Yanghao Li, Piotr Dollár, and Ross Girshick, “Masked autoencoders are scalable vision learners,” in *CVPR*, 2022, pp. 16000–16009.